Molecular tunneling ionization of the carbonyl sulfide molecule by double-frequency phase-controlled laser fields

Hideki Ohmura,[1] Naoaki Saito,[1] and Toru Morishita[2]

[1]*National Institute of Advanced Industrial Science and Technology (AIST), 1-1-1 Higashi, Tsukuba, Ibaraki 305-8565, Japan*

[2]*Department of Engineering Science, University of Electro-Communications, 1-5-1 Chofu-ga-oka, Chofu-shi, Tokyo 182-8585, Japan*

(Received 21 October 2013; published 13 January 2014)

We have investigated the orientation-selective molecular tunneling ionization of carbonyl sulfide (OCS) molecules induced by linearly polarized double-frequency phase-controlled laser fields consisting of a fundamental and a second-harmonic light with a pulse duration of 130 fs and an intensity of 5×10^{13} W/cm^2. We performed simultaneous measurements using gas mixtures of OCS and carbon monoxide to calibrate the relative phase difference of the phase-controlled fields and to verify the mechanism of the tunnel ionization. It is demonstrated that there is a definite correlation between the orientation of ionized molecules and the structure of the highest occupied molecular orbital. We have discussed the experimental results by means of the weak field asymptotic theory. In addition, we have analyzed the quantum dynamics of photoelectrons in simultaneous ion-electron detection. The experimental results can be explained by a two-step model including the interaction with the parent ion. The recollision process plays a minor role for determining the preferable directions of polar molecules in the tunneling ionization at the experimental laser intensity used.

DOI: 10.1103/PhysRevA.89.013405 PACS number(s): 32.80.Qk, 42.50.Hz

I. INTRODUCTION

The highly nonlinear optical response of atoms and molecules has been intensely investigated because of recent progress in techniques to generate intense, ultrashort laser pulses. In nonresonant photoionization processes, an increase in laser intensity causes a transition from multiphoton ionization (MPI) to tunneling ionization (TI); the latter occurs when the laser field suppresses the binding potential of the electron so strongly that the wave function of the outermost electron penetrates and escapes the tunneling barrier [1–7]. Recent studies have revealed that TI occurs mainly in the attosecond (1 as $= 10^{-18}$ s) time region, when the electric field of the laser reaches its maximum value because of a highly nonlinear optical response [8,9]. Analogous to scanning tunneling microscopy (STM), where quantum-tunneling phenomena are applied to observe atomic-scale objects in the space domain, the use of TI induced by intense laser fields enables us to observe ultrafast phenomena in the time domain. Therefore, TI is one of the most important and fundamental phenomena for measuring and controlling physics in the attosecond time regime [10–12].

For atomic TI the so-called Ammosov-Delone-Krainov (ADK) theory [3] is often used to compare the absolute values and electric field dependence of ionization rates between theory and experiment. The ADK model has been extended by Tong and Lin to treat molecular systems [13,14]. At first glance, a qualitative consequence of the molecular ADK model is that the TI rate reflects the geometric structure of the highest occupied molecular orbital (HOMO) [15–19]. Namely, more photoelectrons are extracted via tunneling from the large-amplitude lobe of the HOMO along the opposite direction of the electric field vector. As a consequence of the angular dependence of the TI rate, molecules aligned in a certain direction are selectively ionized in a randomly oriented gas-phase molecular ensemble, and the photofragment-emission pattern induced by molecular TI reflects the asymptotic structure of the molecular orbital [15,16]. As examples of homonuclear diatomic molecules, a butterfly-shaped pattern reflecting the structure of the π orbital in O_2 molecules and a dumbbell-shaped pattern reflecting the σ orbital structure in N_2 molecules have been observed in two-dimensional (2D) photofragment-emission pattern imaging [15]. On the contrary for heteronuclear molecules with asymmetric structures, control of the molecular orientation or orientation-selective measurement is required to discriminate the head-tail order of the molecules. (In general, alignment does not discriminate between the head-tail order of molecules, whereas orientation does discriminate.) Recent TI experiments on carbon monoxide (CO), which has an asymmetric structure [its HOMO is shown in Fig. 1(b)], induced by intense double-frequency phase-controlled laser fields consisting of a fundamental light and its second-harmonic light (hereafter, the $\omega + 2\omega$ laser fields) [20,21], and cold target recoil ion momentum spectroscopy (COLTRIMS) [22] has demonstrated that more tunneling ionization was observed from the C side with a large-amplitude lobe of HOMO than the O side (see Fig. 1).

Recently, however, a molecule with asymmetric structure that shows a different trend to the asymptotic structure of HOMO has been studied [23–25]. The angular dependence of the TI rate for carbonyl sulfide (OCS) molecules [its HOMO is shown in Fig. 1(a)] shows that the ionization rate is maximum when the laser field points from nuclei O to S [Fig. 1(a)], indicating that more tunneling ionization occurs from the O side having a smaller amplitude of HOMO. This has been attributed to the linear Stark shift of the ionization potential. The Stark effect reduces or raises the ionization potential when the laser-field vector is parallel or antiparallel to the permanent dipole of HOMO, leading to a maximum ionization rate for the antiparallel configuration, where more electrons are ionized from the smaller-amplitude side of the HOMO. Namely, the effect of the Stark shift provides the opposite trend to that of the asymptotic amplitude of the HOMO [23–25].

Moreover, the situation for OCS molecules has been found to be somewhat complicated. The angular dependence of the TI rate for OCS is dependent on the laser polarization for

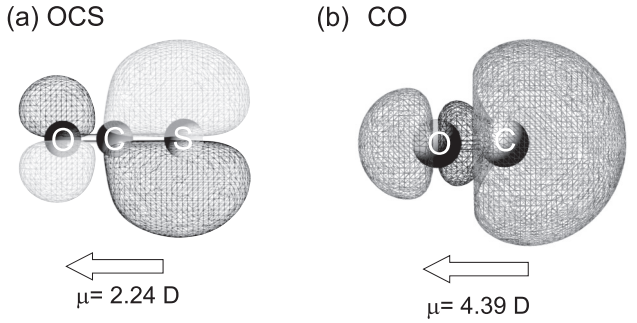

FIG. 1. Molecular structures and isocontours of the highest occupied molecular orbitals (HOMOs) of (a) OCS and (b) CO determined by *ab initio* calculations using the GAUSSIAN 03W software package [method: MP2; basis sets: 6-311++G(3*df*,2*pd*)]. The shadings indicate the signs of the wave functions. The direction of the orbital dipoles is shown by the thick arrows.

both circularly polarized (CP) and linearly polarized (LP) fields [26]. For TI of OCS with single-frequency CP laser fields it was found that maximum ionization occurs when the electric field points along the permanent dipole moment, i.e., along the molecular axis [23–25], whereas for TI of OCS with single-frequency LP laser fields it was found that the ionization yield is maximum when the field is perpendicular to the molecular axis [26]. They discuss the possibility that the discrepancy is caused by the recollision of ionized electrons with the parent ions or by electronically excited states in the multiphoton ionization process [26]. At present, this question remains unanswered.

Meanwhile a theory, called the weak field asymptotic theory (WFAT), based on the Siegert states in a static electric field has been developed within the single active electron approximation [27]. In the WFAT, the solution to the Schrödinger equation is described by the asymptotic expansion with respect to the field strength, treating the Stark effect rigorously. In this theory the TI rate is factorized into a simple product of two parts: One depends only on the target structure and the other on the field strength. It is also shown that the dominance of either the Stark shift or the shape of the HOMO depends on molecules and cannot be determined by just looking at the shape of the HOMOs. Using accurate Hartree-Fock wave functions, a larger TI rate is found from the C side for CO dominated by the Stark shift, indicating that further experimental and theoretical studies including multielectron effects are needed [28].

In this paper, we investigate orientation-selective molecular TI (OSM-TI) of OCS by using double-frequency LP laser fields to obtain more information in addition to that from single-frequency LP and CP laser fields. Simultaneous detection of photofragment ions and photoelectrons from OSM-TI has been performed to track the ground-state orbital and quantum dynamics of photoelectrons from their phase-dependent behaviors. The results obtained by the LP phase-controlled $\omega + 2\omega$ laser fields suggest that TI is dominated by the asymptotic amplitude of HOMO (when the electric field points opposite to the permanent dipole), which is different from the results obtained from both single-frequency LP and CP fields.

II. EXPERIMENT

The total electric field of an LP laser field consisting of two frequencies, the fundamental (ω) and its second harmonic (2ω), is given by $E(t) = E_1\cos(\omega t) + E_2\cos(2\omega t + \phi)$, where E_1 and E_2 are the amplitudes of the electric fields and ϕ is the relative phase difference between the fundamental and its second harmonic. The amplitude of the electric field in the positive (negative) direction is twice that in the negative (positive) direction when $\phi = 0\,(\pi)$ and $E_1 = 2E_2$ [20,29–32].

In general, a single-frequency LP laser field—with a wave form that is symmetric with respect to the negative and positive directions along the laser polarization—cannot discriminate the head-tail order of molecules because the ionization rate of molecules with negative orientation along the direction of polarization is equal to the rate of those with positive orientation. In contrast, the asymmetric wave form of a double-frequency LP $\omega + 2\omega$ laser field can selectively ionize molecules while discriminating the head-tail order of molecules with asymmetric structure if the relevant ionization is a *nonlinear process* such as TI. We have experimentally demonstrated that OSM-TI is induced as a consequence of the directionally asymmetric TI of molecules with an asymmetric HOMO [20,29–31].

The experimental apparatus, which has been described previously [20], consisted of a Ti:sapphire laser system, a robust phase-controlled $\omega + 2\omega$ laser-field generator, and a time-of-flight mass spectrometer (TOF-MS) designed for simultaneous ion-electron detection equipped with a supersonic molecular beam source. Briefly, the output beam of the Ti:sapphire laser system (800-nm wavelength, 130-fs duration, 1.0-mJ/pulse pulse energy, 20-Hz repetition rate) was delivered to the robust phase-controlled $\omega + 2\omega$ laser-field generator. With this optics set, we could control the relative phase difference ϕ between the ω and 2ω pulses by using a rotatable 10-mm-thick quartz plate with a resolution of about 30 as (0.05π) after second-harmonic generation (β-barium borate, type I phase matching, 1-mm thickness, conversion efficiency: 30%). The ratio I_2/I_1 was adjusted to around 0.25 ($E_2/E_1 = 0.5$), where I_1 and I_2 are the intensities of the ω and 2ω pulses, respectively. The phase-controlled $\omega + 2\omega$ laser beam was focused on a supersonic molecular beam of OCS or CO, which was used as a reference molecule [diluted (5%) with He gas], in the TOF-MS by an aluminum concave mirror (200-mm focal length). We estimated the total intensity $I = I_1 + I_2$ to be approximately 5×10^{13} W/cm^2 ($I_1 = 4 \times 10^{13}$, $I_2 = 1 \times 10^{13}$ W/cm^2) at the focus. The ionization potential and orbital dipole (HOMO) of OCS are 11.18 eV and 2.24 D, whereas those of CO are 14.0 eV and 4.39 D.

The TOF-MS, designed for simultaneous ion-electron detection, consisted of a Wiley–McLaren-type two-stage accelerator, field-free drift tubes for electrons and ions, and two opposing position-sensitive detectors. Photofragment ions and photoelectrons produced by the $\omega + 2\omega$ pulses were each accelerated by static electric fields toward one of the opposing detectors. After passing through a drift tube, the photofragment ions and photoelectrons were detected by position-sensitive detectors composed of a microchannel plate (MCP) with a phosphor screen (77-mm diameter). The two-dimensional (2D) angular distributions of photofragment ions and photoelectrons acquired from each position-sensitive detector were

recorded by a charge-coupled device (CCD) camera system. Mass selectivity of the fragment ions for the 2D images was achieved by gating the gain of the detector (temporal width: 100 ns) at the arrival time of each photofragment ion.

We use the definition of the experimental configuration based on the polarization direction, the detection axis, and the direction of the electric field maxima at relative phase difference $\phi = 0$ reported in [20]. In the measurement of one-dimensional (1D) TOF spectra, the polarization direction of the $\omega + 2\omega$ laser fields is set to be horizontal and parallel to the detection axis, and we define $\phi = 0$ to be the condition when the electric field maximum points toward the ion detector (forward/backward configuration). In this configuration, we could simultaneously measure the phase dependence of all photofragment ions under identical conditions of the relative phase difference ϕ and laser intensity. In the measurement of the 2D photofragment (photoelectron) angular distribution, the polarization direction of the $\omega + 2\omega$ laser fields is set to be horizontal and perpendicular to the detection axis, and we define $\phi = 0$ to be the condition when the electric field maximum points leftward (rightward) with respect to the ion (electron) detector (leftward-rightward configuration). In this configuration, we could simultaneously measure the phase dependence of both the mass-selected photofragment ions and the photoelectrons under identical conditions of the relative phase difference ϕ and laser intensity. To calibrate the relative phase difference ϕ, we performed a simultaneous measurement using gas mixtures of target molecules and reference CO molecules [30] in the forward-backward configuration. This method provides an accurate phase relationship between target molecules and reference molecules under identical experimental conditions, i.e., within the same experimental run.

III. RESULTS AND DISCUSSION

Figure 2(a) shows the kinetic energy spectra and the leftward-rightward yield ratio (I_L/I_R) as a function of the relative phase difference and kinetic energy for OC^+ (upper panel) and S^+ (lower panel) photofragment ions when OCS molecules were irradiated with $\omega + 2\omega$ pulses. The kinetic energy spectra of the photofragment ions in Fig. 2(a) were obtained from the inset images of 2D angular distributions of photofragment ions along the laser polarization direction. Pronounced angular localizations along the laser polarization were observed in the 2D distributions of the photofragment ions [Fig. 2(a) insets].

Clear periodicities of 2π were observed in I_L/I_R as a function of ϕ for both OC^+ and S^+ [Fig. 2(b)]. The phase dependence between OC^+ and S^+ indicates that they were completely out of phase with each other. This result shows that phase-controlled $\omega + 2\omega$ pulses can discriminate the molecular orientation of the head-tail order. The phase-dependent behaviors of both OC^+ and S^+ are not dependent on the kinetic energy [Fig. 2(b)]. The fact that OC^+ (S^+) ions produced various dissociation channels such as $OCS^+ \rightarrow OC^+ + S$, $OSC^+ \rightarrow OC + S^+$, and $OCS^{2+} \rightarrow OC^+ + S^+$ indicates that leftward-rightward asymmetries do not originate from the difference of the dissociation channels but from the orientation of ionized molecules.

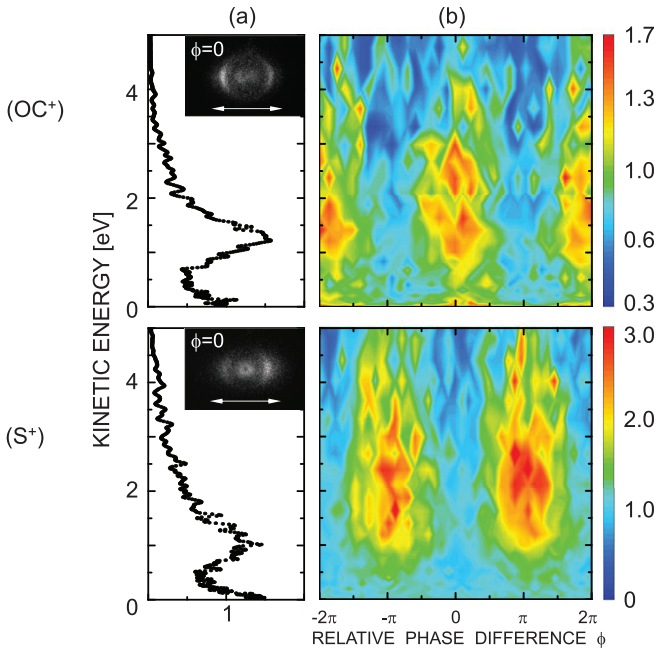

FIG. 2. (Color) (a) Kinetic energy spectra and (b) density plots of the leftward-rightward yield ratio (I_L/I_R) as a function of the relative phase difference ϕ and kinetic energy for OC^+ photofragment ions (upper panel) and S^+ photofragment ions (lower panel) produced from OCS molecules irradiated with the phase-controlled $\omega + 2\omega$ laser fields. The kinetic energy spectra in (a) were obtained from the inset images of the 2D angular distributions of photofragment ions at $\phi = 0$. The double-headed arrows indicate the direction of polarization.

Furthermore, the leftward-rightward asymmetries show that the OC^+ (S^+) ions were preferentially emitted to the left (right) of the detector at $\phi = 0$, when the electric field maximum pointed to the left. Conversely, the directional asymmetries of each of the photofragment ions were reversed at $\phi = \pi$. This result shows that electrons are much more strongly extracted from the large-amplitude part of the HOMO at the field maxima of the $\omega + 2\omega$ laser fields.

We note that in our experiment we do not explicitly measure the angular dependence of the TI rate. If ideal molecular TI occurs in the deep tunneling regime, a butterfly-shaped pattern reflecting the structure of the π orbitals should be observed in the 2D photofragment emission. It is known that laser pulses with durations of more than 100 fs increasingly induce dynamic molecular alignment (not orientation) by the torque generated by the interaction between the laser field and the induced dipole within the laser pulse duration [15]. Almost all molecules experience some contribution of dynamic molecular alignment due to an induced dipole. Therefore, the 130-fs $\omega + 2\omega$ pulse in this experiment induces dynamic alignment, and thus our measurement is a result of the OSM-TI in aligned molecules during the laser pulse rather than in randomly oriented molecules.

As an additional experiment to calibrate the relative phase difference ϕ, and to verify the mechanism of OSM-TI regardless of the orientation of the detected molecules, we performed simultaneous measurements using gas mixtures of OCS and CO as a reference in the forward-backward

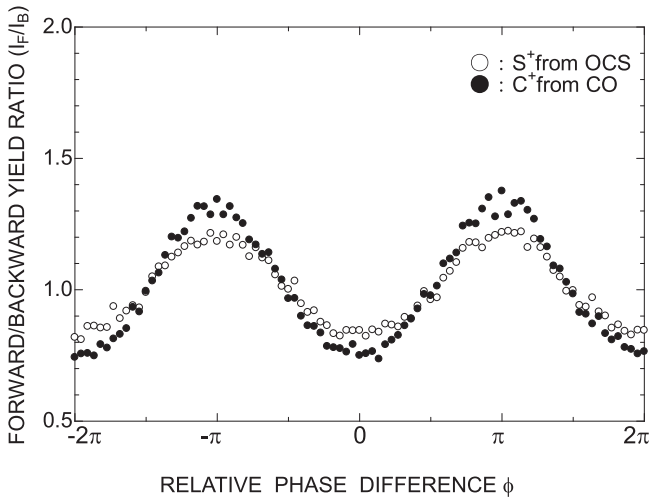

FIG. 3. Forward-backward yield ratio (I_F/I_B) using gas mixture of OCS-CO as a function of the relative phase difference ϕ: (open circles) S^+ produced from OCS and (closed circles) C^+ produced from reference CO.

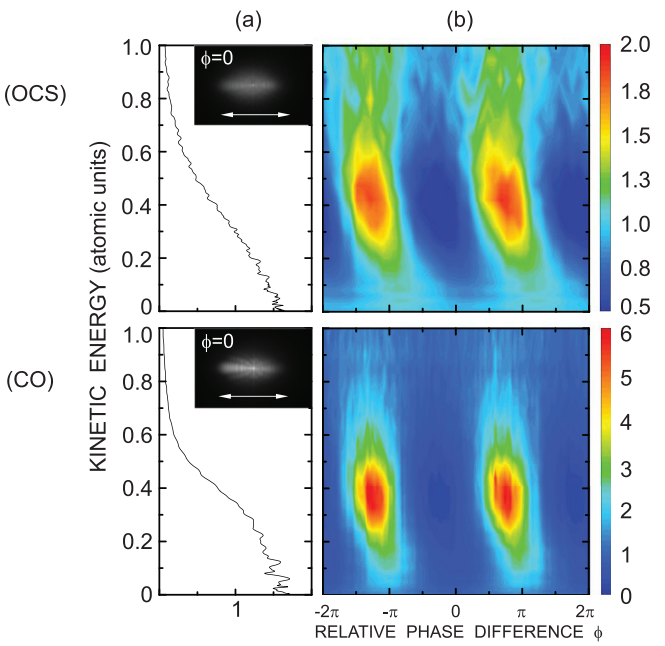

FIG. 4. (Color) (a) Kinetic energy spectra and (b) density plots of the leftward-rightward yield ratio (I_L/I_R) as a function of the relative phase difference ϕ and kinetic energy of photoelectrons produced from OCS (upper panel) and CO (upper panel) irradiated with phase-controlled $\omega + 2\omega$ laser fields. The kinetic energy spectra (a) were obtained from the inset images of 2D angular distributions of photoelectrons at $\phi = 0$. The double-headed arrows indicate the direction of polarization.

configuration [20,30]. Recent experiments on CO by using phase-controlled $\omega + 2\omega$ laser fields [20,21] and COLTRIMS [23] have confirmed that more electrons are extracted from the C side with the large-amplitude lobe of the HOMO than the O side. Figure 3 shows the forward-backward yield ratio I_F/I_B of C^+ generated from CO, and S^+ generated from OCS, as functions of the relative phase difference ϕ using the gas mixture OCS-CO. Because C^+ generated from CO could interfere with that generated from OCS in the TOF spectrum, we minimized the contribution of C^+ from OCS below 20% of the total C^+ signal intensity by adjusting the ratio of partial pressures between OCS and CO in the gas mixture. We also carefully checked that the phase dependence of C^+ is solely caused by CO and not by OCS. The S^+ generated from OCS and the C^+ generated from CO were completely in phase with each other. (The relative phase difference ϕ in this paper was calibrated by the result shown in Fig. 3.) As shown in Fig. 1, we have experimentally confirmed that there is a definite correlation between the orientation of detected molecules and the geometric structure of the HOMO when the LP $\omega + 2\omega$ laser field is used. It has been reported that the contribution of HOMO-1 [33,34] to TI for CO was ~30% of the total signal with a laser intensity about ten times higher than that used in our experiments [22]. The contribution of HOMO-1 seems to have been much smaller in the present study.

Simultaneous ion-electron detection enables us to track the quantum dynamics of photoelectrons by using phase-dependent oriented molecules as a phase reference [20]. Figure 4(a) shows the kinetic energy spectra and the leftward-rightward yield ratio (I_L/I_R) of photoelectrons as functions of the relative phase difference and kinetic energy generated from OCS (upper panel) and reference CO taken from [20] (lower panel). The kinetic energy spectra of the photoelectrons in Fig. 4(a) were obtained from the inset images of 2D angular distributions of photoelectrons along the laser polarization direction. Pronounced angular localizations along with the laser polarization were observed in the 2D distributions of the photoelectrons [Fig. 4(a) insets]. In the corresponding photoelectron spectrum in Fig. 4(a), the energy distribution shows a broad and exponentially decreasing dependence, indicating that the laser intensity reaches the TI regime. Clear periodicities of 2π were observed in the I_L/I_R ratio from both OCS and CO. The phase-dependent behaviors of photoelectrons were dependent on photoelectron kinetic energy. The same tendency exists between OCS and CO, which can be divided into two regions: slow photoelectrons (0–0.3 a.u.), with directional asymmetry around $\phi = \pi$ (0), and fast photoelectrons (0.3–0.7 a.u.), with directional asymmetry around $\phi = \pi/2$ ($3\pi/2$) [20].

We now discuss the molecular TI of OCS from the standpoint of the quantum dynamics of the phase-dependent photoelectrons generated by the $\omega + 2\omega$ laser fields. In our previous study of CO molecules, we reported that the quantum dynamics of photoelectrons generated by the $\omega + 2\omega$ field could be explained by a two-step model that consists of quasistatic TI and the following of the motion of photoelectrons driven by $\omega + 2\omega$ laser fields in the potential of the parent ion based on a semiclassical approach [20,35–37]. The phase-dependent behavior of the slow photoelectrons is in good agreement with the two-step model including the core effects. This result can be explained by the effect in which slow photoelectrons are emitted toward the counterintuitive direction because of the strong attraction of the parent ion [20,36,37]. Then, the effect of the parent ion becomes weaker for the phase-dependent behavior of the fast photoelectrons, and directional

asymmetry at $\phi = \pi/2$ $(3\pi/2)$ is observed [20,36]. This result is consistent because fast photoelectrons, which are less affected by the interaction with the parent ion than slow ones, are driven by the intense $\omega + 2\omega$ laser fields, shaking off the attractive force. We have successfully explained the transition from slow photoelectrons to fast electrons in the phase-dependent behavior of directionally asymmetric photoelectron emission in CO induced by the $\omega + 2\omega$ laser field [20]. We note that the result with the numerical solution to the time-dependent Schrödinger equation is in good agreement with the experiment [20], indicating that the relative phase dependence of photoelectron spectra is not very sensitive for randomly oriented molecules. To clarify this point, further analysis would be required using a time-dependent theory such as the adiabatic theory for ionization [38,39].

Returning to the OCS experimental results, a comparison of the experimental results between CO and OCS shows that they exhibit similar behavior. Therefore, we can safely say that the more electrons are ionized from the S side of OCS with a larger lobe of HOMO and the phase-energy dependence of the generated photoelectrons for OCS can be explained by molecular TI reflecting the geometric structure of the HOMO and the dynamics of photoelectrons driven by $\omega + 2\omega$ laser fields based on the two-step model. We discuss our experimental results with the TI rates with the WFAT which includes the dipole moment of the HOMO rigorously within the single active electron approximation under the weak field limit [40]. For the CO case, the WFAT has more static ionization rates from the O side, which is opposite to the experimental results. Since the WFAT fully contains the information on the TI rates from the HOMO, the main source of the difference between the theory and experiment is due to multielectron effects such as the dipole moment of the core cation of CO^+. Recently a time-dependent Hartree-Fock calculation shows a good agreement with experimental data for a circular polarized light, and the importance of dynamic core polarization effects was discussed [41]. For the OCS case, the TI rate of the WFAT indicates a higher and shaper peak at the O side ($\sim$30°) and lower and broader peak at the S side ($\sim$120°) due to the π-orbital nature of the HOMO; see Fig. 11 in Ref. [40]. We calculated the TI yields from the S side and the O side by summing up the angular dependence of the ionization rate over each of the S side (90°–180°) and the O side (0°–90°) and found that the resulting ratio of $\sim$1.7 is consistent with the experiment. The dynamic core polarization is concluded to be small for the TI of OCS. A comprehensive theory involving multielectron effects for any molecules is ongoing.

Finally, we discuss the differences in the experimental results for TI induced by the single-frequency CP and LP laser fields reported by other groups [23,26] and by the double-frequency LP laser fields in this study.

First, it has been pointed out that in LP laser fields, a tunneled photoelectron recollides with the parent ion by the oscillating laser field, whereas in CP laser fields it does not revisit the parent ion [23,26]. This recollision process induces recombination and rescattering of tunneled photoelectrons, and might induce the deviation from a pure TI process. Considering the laser intensity in the experiments with CO and OCS, the recollision process should make certain contributions, and should be observed as a difference in the phase dependence. However, the observed phase-dependent behavior of the photoelectrons can be explained by the two-step model including the core effect, which does not include the effect of the recollision process [20,36,37]. Therefore, molecular TI reflecting the geometric nature of the HOMO seems to be the main process, and the contribution of the recollision process that could induce deviations from the molecular TI reflecting the geometric nature of the HOMO seems not to be strong enough to reverse the direction of the selectively ionized molecules expected by molecular TI reflecting the geometric nature of the HOMO. The analysis including the rescattering process with the adiabatic theory [38,39] is a challenging task.

Second, it has been pointed out that the difference in experimental results can be attributed to the participation of different intermediate excited states in the ionization process [26,42–44]. The two-step model used in this work is valid in the adiabatic regime where the ratio between atomic and laser time scales (ω/I_p for a monochromatic field) is much smaller than unity [38,39]. Our experimental conditions are in the vicinity of the onset of the adiabatic regime. In other words, in terms of the Keldysh parameter $\gamma \sim 1.1$ is in the boundary between the TI and MPI regimes. Thus other ionization mechanisms, in which excited states play a role, may contribute to the ionization process. In addition to the excited states induced by single-frequency LP laser fields, the LP $\omega + 2\omega$ laser field induces excited states different in parity because of the different selection rules for the one-photon transition of the 2ω photon and the two-photon transitions of the ω photon. Therefore, in this context we can say that the molecular TI for OCS is sensitive to the relevant excited states in the ionization process. However, it remains unclear why the LP $\omega + 2\omega$ laser fields lead to the OSM-TI reflecting the geometric structure of the HOMO. One possible explanation is a quantum interference effect between intermediate excited states [45,46]. Because the relevant intermediate states differ in parity owing to the different selection rules for the one- and two-photon transitions, the interference between the two transitions induces the breaking of spatial symmetry. This interference effect with spatial symmetry breaking might enhance the penetration of the wave function of the outermost electron to the tunneling barrier, leading to OSM-TI. Further theoretical analysis that considers intermediate excited states is required. From an experimental viewpoint, we note that we have observed an enhancement of OSM-TI induced by LP $\omega + 2\omega$ laser pulses with nanosecond duration, where MPI plays a role, rather than femtosecond pulses [31].

IV. CONCLUSION

We investigated the OSM-TI of OCS induced by LP phase-controlled $\omega + 2\omega$ laser fields with a pulse duration of 130 fs and an intensity of 5×10^{13} W/cm^2. We have experimentally confirmed that there is a definite correlation between the orientation of detected molecules and the geometric structure of the HOMO. The orientation of ionized OCS molecules is consistent with that predicted by the recently developed weak field asymptotic theory (WFAT) including the effects of the dipole moment of HOMOs [27,28,40]. More ionization is extracted from the S side of OCS molecule. By comparing the

phase-dependent behavior of photoelectrons between OCS and CO, we analyzed the quantum dynamics of photoelectrons in simultaneous ion-photoelectron detection. The experimental results for OCS, as well as for CO, can be explained by a two-step model including the interaction with the parent ion, and the recollision process plays a minor role to determine the preferable TI directions of polar molecules. A comparison between the present experiment and other experiments [20,24] indicates that molecular TI for OCS is sensitive to the relevant excited states in the ionization process. Because the model used in the work considers only the HOMO and does not include information on intermediate excited states, a TI theory that considers intermediate excited states is required.

ACKNOWLEDGMENTS

This work was supported by a Grant-in-Aid for Challenging Exploratory Research and Scientific Research (B) from the Japan Society for the Promotion of Science.

[1] L. V. Keldysh, Zh. Eksp. Teor. Fiz. **47**, 1945 (1964) [Sov. Phys. JETP **20**, 1307 (1965)].
[2] A. M. Perelomov, N. B. Popov, and M. V. Terent'ev, Zh. Eksp. Teor. Fiz. **50**, 1393 (1966) [Sov. Phys. JETP **23**, 924 (1966)].
[3] M. V. Ammosov, N. B. Delone, and V. P. Krainov, Zh. Eksp. Teor. Fiz. **91**, 2008 (1986) [Sov. Phys. JETP **64**, 1191 (1986)].
[4] F. H. M. Faisal, J. Phys. B **6**, L89 (1973).
[5] H. R. Reiss, Phys. Rev. A **22**, 1786 (1980).
[6] P. B. Corkum, N. H. Burnett, and F. Brunel, Phys. Rev. Lett. **62**, 1259 (1989).
[7] E. Mevel, P. Breger, R. Trainham, G. Petite, P. Agostini, A. Migus, J.-P. Chambaret, and A. Antonetti, Phys. Rev. Lett. **70**, 406 (1993).
[8] M. Uiberacker, Th. Uphues, M. Schultze, A. J. Verhoef, V. Yakovlev, M. F. Kling, J. Raushenberger, N. M. Kabachnik, H. Schröder, M. Lezius, K. L. Kompa, H.-G. Muller, M. J. J. Vrakking, S. Hendel, U. Kleineberg, U. Heinzmann, M. Drescher, and F. Krausz, Nature **446**, 627 (2007).
[9] P. Eckle, A. N. Pfeiffer, C. Cirelli, A. Staudte, R. Dörner, H. G. Muller, M. Büttiker, and U. Keller, Science **322**, 1525 (2008).
[10] T. Brabec and F. Krausz, Rev. Mod. Phys. **72**, 545 (2000), and references therein.
[11] P. B. Corkum and F. Krausz, Nat. Phys. **3**, 381 (2007), and references therein.
[12] F. Krausz and M. Ivanov, Rev. Mod. Phys. **81**, 163 (2009), and references therein.
[13] X. M. Tong, Z. X. Zhao, and C. D. Lin, Phys. Rev. A **66**, 033402 (2002).
[14] C. D. Lin and X. M. Tong, J. Photochem. Photobiol., A **182**, 213 (2006).
[15] A. S. Alnaser, S. Voss, X.-M. Tong, C. M. Maharjan, P. Ranitovic, B. Ulrich, T. Osipov, B. Shan, Z. Chang, and C. L. Cocke, Phys. Rev. Lett. **93**, 113003 (2004).
[16] A. S. Alnaser, C. M. Maharjan, X. M. Tong, B. Ulrich, P. Ranitovic, B. Shan, Z. Chang, C. D. Lin, C. L. Cocke, and I. V. Litvinyuk, Phys. Rev. A **71**, 031403(R) (2005).
[17] D. Pavičić, K. F. Lee, D. M. Rayner, P. B. Corkum, and D. M. Villeneuve, Phys. Rev. Lett. **98**, 243001 (2007).
[18] A. Staudte, S. Patchkovskii, D. Pavičić, H. Akagi, O. Smirnova, D. Zeidler, M. Meckel, D. M. Villeneuve, R. Dörner, M. Yu. Ivanov, and P. B. Corkum, Phys. Rev. Lett. **102**, 033004 (2009).
[19] S. Petretti, Y. V. Vanne, A. Saenz, A. Castro, and P. Decleva, Phys. Rev. Lett. **104**, 223001 (2010).
[20] H. Ohmura, N. Saito, and T. Morishita, Phys. Rev. A **83**, 063407 (2011).
[21] H. Li, D. Ray, S. De, I. Znakovskaya, W. Cao, G. Laurent, Z. Wang, M. F. Kling, A. T. Le, and C. L. Cocke, Phys. Rev. A **84**, 043429 (2011).
[22] J. Wu, L. Ph. H. Schmidt, M. Kunitski, M. Meckel, S. Voss, H. Sann, H. Kim, T. Jahnke, A. Czasch, and R. Dörner, Phys. Rev. Lett. **108**, 183001 (2012).
[23] L. Holmegaard, J. L. Hansen, L. Kalhøj, S. L. Kragh, H. Stapelfeldt, F. Filsinger, J. Küpper, G. Meijer, D. Dimitrovski, M. Abu-samha, C. P. J. Martiny, and L. B. Madsen, Nat. Phys. **6**, 428 (2010).
[24] D. Dimitrovski, C. P. J. Martiny, and L. B. Madsen, Phys. Rev. A **82**, 053404 (2010).
[25] D. Dimitrovski, M. Abu-samha, L. B. Madsen, F. Filsinger, G. Meijer, J. Küpper, L. Holmegaard, L. Kalhøj, J. H. Nielsen, and H. Stapelfeldt, Phys. Rev. A **83**, 023405 (2011).
[26] J. L. Hansen, L. Holmegaard, J. H. Nielsen, H. Stapelfeldt, D. Dimitrovski, and L. B. Madsen, J. Phys. B: At. Mol. Opt. Phys. **45**, 015101 (2012).
[27] O. I. Tolstikhin, T. Morishita, and L. B. Madsen, Phys. Rev. A **84**, 053423 (2011).
[28] L. B. Madsen, O. I. Tolstikhin, and T. Morishita, Phys. Rev. A **85**, 053404 (2012).
[29] H. Ohmura, N. Saito, and M. Tachiya, Phys. Rev. Lett. **96**, 173001 (2006).
[30] H. Ohmura, F. Ito, and M. Tachiya, Phys. Rev. A **74**, 043410 (2006).
[31] H. Ohmura and M. Tachiya, Phys. Rev. A **77**, 023408 (2008).
[32] H. Ohmura, N. Saito, H. Nonaka, and S. Ichimura, Phys. Rev. A **77**, 053405 (2008).
[33] B. K. McFarland, J. P. Farrell, P. H. Bucksbaum, and M. Gühr, Science **322**, 1232 (2008).
[34] H. Akagi, T. Otobe, A. Staudte, A. Shiner, F. Turner, R. Dörner, D. M. Villeneuve, and P. B. Corkum, Science **325**, 1364 (2009).
[35] D. W. Schumacher, F. Weihe, H. G. Muller, and P. H. Bucksbaum, Phys. Rev. Lett. **73**, 1344 (1994).
[36] A. D. Bandrauk and S. Chelkowski, Phys. Rev. Lett. **84**, 3562 (2000).
[37] S. Chelkowski, M. Zamojski, and A. D. Bandrauk, Phys. Rev. A **63**, 023409 (2001).
[38] O. I. Tolstikhin, T. Morishita, and S. Watanabe, Phys. Rev. A **81**, 033415 (2010).
[39] O. I. Tolstikhin and T. Morishita, Phys. Rev. A **86**, 043417 (2012).

[40] L. B. Madsen, F. Jensen, O. I. Tolstikhin, T. Morishita, A. Migus, J. P. Chambaret, and A. Antonetti, Phys. Rev. A **87**, 013406 (2013).
[41] B. Zhang, J. Yuan, and Z. Zhao, Phys. Rev. Lett. **111**, 163001 (2013).
[42] V. Kumarappan, L. Holmegaard, C. Martiny, C. B. Madsen, T. K. Kjeldsen, S. S. Viftrup, L. B. Madsen, and H. Stapelfeldt, Phys. Rev. Lett. **100**, 093006 (2008).
[43] M. Abu-samha and L. B. Madsen, Phys. Rev. A **80**, 023401 (2009).
[44] E. Penka Fowe and A. D. Bandrauk, Phys. Rev. A **84** 035402 (2011).
[45] Y. Y. Yin, C. Chen, D. S. Elliott, and A. V. Smith, Phys. Rev. Lett. **69**, 2353 (1992).
[46] Z.-M. Wang and D. S. Elliott, Phys. Rev. Lett. **87**, 173001 (2001).